

Carrier-Envelope Phase Sensitive Photoelectron Emission Induced by Sub-10-fs Laser Pulses

Péter Dombi¹ and Győző Farkas²

¹ Institut für Photonik, Technische Universität Wien

Gusshausstr. 27, A-1040 Wien, Austria; E-mail: dombi@tuwien.ac.at

² KFKI Research Institute for Solid State Physics

P.O. Box 49, H-1525 Budapest, Hungary

Received 3 March 2005

Abstract. We present a simple phenomenological model and its consequences for explaining the recently observed sensitivity of multi-photon-induced surface photoelectron emission to the carrier-envelope phase of a laser pulse. We discuss the limitations of the model suggested by time-resolved measurements of the photoelectron emission process induced by sub-10-fs laser pulses giving thus new insight into the only laser–solid interaction process studied by controlled optical waveforms so far.

Keywords: carrier-envelope phase, multi-photon photoemission, ultrafast dynamics, femtosecond lasers

PACS: 79.60.Bm, 73.50.Fq, 79.20.Ds, 42.65.Re

1. Introduction

Sub-10-fs laser pulses have gained immense importance in the past decade. The generation of such pulses relies on Ti:sapphire laser technology due to its solid-state-based nature (and the resulting compactness) and extremely wide gain bandwidth of the laser host material. These oscillators and amplified laser systems have been used as workhorse systems for ultrafast time-resolved, pump-probe etc., studies in various fields of basic research and applied science. The characteristic timescale of several outer shell atomic electron excitation processes lies in the sub-10-fs range enabling researchers to observe a brand new behaviour of these well-known processes just by substituting the conventional sub-100-fs sources inducing the process with sub-10-fs ones [1].

The most well-known example is the generation of high-order extreme ultraviolet (XUV) harmonics of the near infrared Ti:sapphire laser pulse in noble gas media.

The usage of 5–6 fs pulses to induce this effect (already known for two decades) resulted in the first-ever proof of the existence of isolated attosecond pulses [2]. Even though generation mechanisms were well known after the first pioneering paper more than ten years ago [3], still, significant improvement of Ti:sapphire technology was needed to make such experiments possible (including e.g. the application of chirped mirrors [4] for external pulse compression), since typically few-cycle laser pulses with mJ pulse energies are needed to generate isolated attosecond pulses. This single experimental step [2] immediately opened the door to exploring electron dynamics on the sub-fs timescale previously inaccessible to researchers in a controlled manner with any method whatsoever [5]. Attosecond metrology and spectroscopy brought several breakthrough observations in basic atomic physics in the past 2–3 years and the wealth of potential applications and benefits makes this an attractive research field in the future, too (for an extensive review see Ref. [5] and references therein).

Besides high harmonic generation another, experimentally not yet explored field of the application of sub-10-fs laser pulses could be the generation of monoenergetic electron beams by laser wake field acceleration [6]. This holds the potential of large-scale particle physics facilities being substituted with table-top laser systems. The state-of-the-art is the generation of monoenergetic electron beams with >100 MeV energies, however, recent breakthrough experiments were carried out using relatively long, 30–40 fs laser pulses [6]. Provided that a terawatt-scale laser system is constructed delivering 5 fs laser pulses with the desired high prepulse contrast brand new effects could be observed in laser-driven electron acceleration [7], especially, when one uses controlled optical waveforms.

The major breakthrough in terms of Ti:sapphire laser technology development in the past years, however, was not just a step forward in the everlasting quest for shorter and shorter pulses (with the current record being 2.8 fs in the visible spectral domain corresponding merely to a single optical cycle at the Ti:sapphire central wavelength of 800 nm [8]), but control of the so-called carrier-envelope (CE) phase of the laser pulse itself [9]. This quantity denotes the relative phase between the envelope of the laser pulse and its carrier wave (see Fig. 1), and appears as φ in the equation $E_L(t) = A_L(t) \cos(\omega_L t + \varphi)$ describing the electric field evolution of the transform-limited pulse with envelope $A_L(t)$. Sometimes it is also referred to as the “absolute” phase with a certain degree of imprecision. In a mode-locked output pulse train of a laser oscillator the CE phase value is shifted by a certain amount from pulse-to-pulse (this amount is to be denoted by $\Delta\varphi$) due to the difference between the phase velocity and the group velocity of the pulse within the oscillator. The amount of this phase shift can be quantified by the equation $\Delta\varphi = 2\pi f_{\text{ceo}}/f_r$, where f_r is the repetition rate of the oscillator and f_{ceo} denotes the so-called carrier-envelope offset frequency which is directly measurable with the aid of a recently found self-referencing method called f -to- $2f$ (or ν -to- 2ν) interferometry [9]. This way this seemingly random pulse-to-pulse CE phase shift (rooted in thermal and mechanical instabilities, pump laser intensity fluctuations and air movement within the laser oscillator) can be stabilized by locking f_{ceo} to an external reference. With

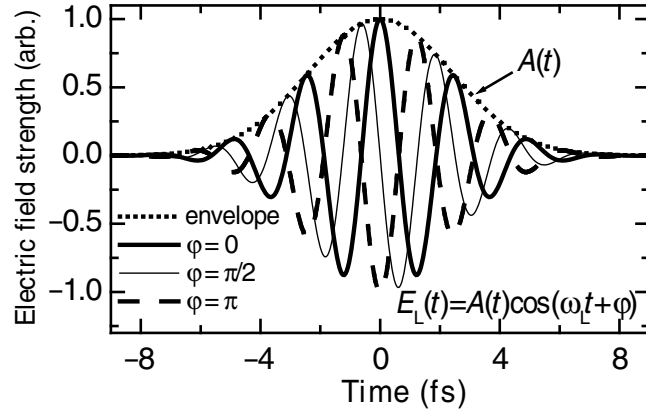


Fig. 1. Different possible evolutions of the electric field $E_L(t)$ of few-cycle laser pulses having the same pulse envelope (pulse intensity envelope length, $\tau_L = 4$ fs FWHM, $\lambda_0 = 750$ nm, Gaussian pulse shape: $A_L(t) = A_0 \exp(-2t^2 \ln 2 / \tau_L^2)$). In case of a transform-limited pulse, once the envelope is fully characterized one needs only a single further parameter, the carrier-envelope phase (φ) to fully determine the electromagnetic waveform. We depicted a *cosine* ($\varphi = 0$), a *sine* ($\varphi = \pi/2$) and a *minus cosine* pulse ($\varphi = \pi$)

a certain method this can be even zero frequency, which means that each pulse coming from the oscillator has the same waveform.

The inherent drawback of this method is that it is not sensitive to the actual value of the CE phase, φ itself, but it only assesses its pulse-to-pulse shift, $\Delta\varphi$. The actual value of the CE phase for each laser pulse, however, proved to be decisive for example for the reproducible generation of attosecond XUV pulses. If the generating laser pulse is a so-called cosine pulse ($\varphi = 0$) with 5–6 fs duration, a single attosecond burst emerges from the noble gas jet target. Contrarily, a similar sine pulse ($\varphi = \pi/2$) results in a double burst, which is not particularly beneficial for an attosecond pump-probe experiment [10]. Therefore, any kind of physical effect would bring benefits to attosecond applications that can measure the CE phase value of a laser pulse on a single-shot basis using only a portion of the beam (preferably using only pulses with nJ pulse energy) and a simple set-up.

The only demonstrated candidate to date is multi-photon-induced photoelectron emission from a metal surface, raising interest due to its potential use in the above-mentioned application [11–14]. However, sophisticated and difficult-to-track simulations based on the jellium model of metals and density functional theory predicted CE phase sensitivities [11] orders of magnitude higher than the observed ones [12, 13]. This discrepancy is still waiting to be removed. Therefore we present a simple phenomenological model that is capable of explaining not just the CE phase sensitivity of photoelectron emission, but it is also suitable for making quantitative

predictions on the extent of this effect. We examine the role of pulse length within the framework of this picture and compare the quantitative predictions to that of Refs. [11] and [13]. We also present a time-resolved measurement that can explain why the observed CE phase sensitivity is much lower than the one predicted by both the jellium-based and the phenomenological model and show the way of incorporating the effects responsible for this into the framework of our phenomenological model.

2. A Phenomenological Model for CE Phase Sensitive Photoelectron Emission

Our approach is inspired by the simple and easy-to-visualize three-step semiclassical model of high harmonic generation from Corkum [15] the consequences of which are in remarkable agreement with the results of rigorous quantum mechanical treatment of the process [16]. In that case of gas-phase atomic ionization induced by the field of a laser pulse the electron is assumed to be “born” in the continuum with zero initial velocity after tunnelling through the potential barrier distorted by the laser field. After this it is treated as a free particle and its movement is examined in the potential of the laser field only. Provided that the beam is linearly polarized the electron wave packet returns to its parent ion after a certain wiggly motion in the laser field and recombines with the ion with some finite probability. The result is the emission of high-harmonic photons. Their energy is determined by the ponderomotive potential and the binding energy. Obviously, the time of birth, the instant of this recombination, and consequently the temporal and spectral characteristics of the XUV emission are also influenced by the carrier-envelope phase of the laser pulse if the generating pulses have few-cycle duration. The main reason is that the participating physical processes are directly governed by the laser field not just the intensity evolution of the pulse.

A somewhat analogous picture can be constructed for multi-photon-induced photoelectron emission from solid surfaces (MSPE). The first step corresponds to instantaneous electron emission as a result of which a free electron is “born” somewhere near the metal surface. We can assume that the probability of the emission is proportional to $A_L(t)^{2n}$, with n being the order of the process, according to the perturbative nature of MSPE and well-known, justified intensity dependence laws that were found to be valid down to the few-cycle regime [12, 14].

The second step is determining the motion of the electron near the surface influenced only by the laser field and the mirror charge potential. The effect of this latter potential can be neglected according to numerical proofs. During its motion the field evolution will either push the electron back into the surface either immediately or after performing a wiggly motion in the laser field (see the inset of Fig. 2). For simplicity let us take a few-cycle laser pulse and an electron that is released exactly at the peak of the intensity envelope of this pulse. In this case it is obviously not unimportant in terms of the end result what CE phase the pulse actually has.

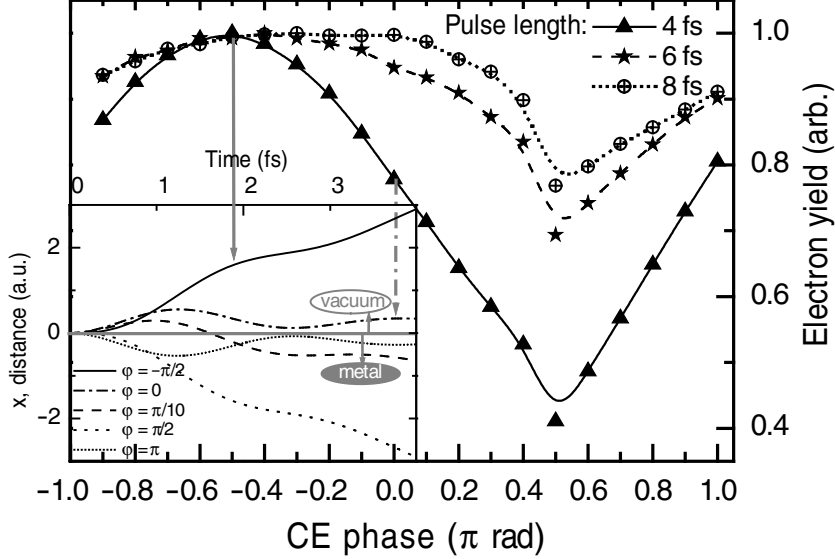


Fig. 2. Computed charge emitted from a gold surface (modelled according to the phenomenological model described in Section 2) exposed to a Gaussian laser pulse ($\lambda_0 = 750$ nm) with intensity in the perturbative limit plotted as a function of the CE phase φ . The parameter for the set of curves is the pulse duration, ranging from 4 fs to 8 fs. The light is incident with the electric field oriented along the surface normal ('P' polarization, grazing incidence). The inset shows classically computed free electron trajectories assuming instantaneous electron emission at the peak of a 4 fs pulse and subsequent classical motion in vacuum governed by the electric field only. For some representative trajectories ($\varphi = \pi/10$, $\varphi = \pi/2$, $\varphi = \pi$) the electron is steered back to the surface (represented by the $x = 0$ line) not being able to escape. The CE phase sensitivity of the emission process is rooted in this phenomenon. The trajectories corresponding to some data points in the main graph are marked by arrows

For the range of $-\pi/2 < \varphi < 0$ it is driven away from the surface and allows to be collected by e.g. a detection electrode. Out of this range the field pushes it towards the surface in the manner described above. It has to be noted that the centre of this interval is in remarkable agreement with the predicted maximum of electron yield as a function of the CE phase using a complicated jellium-like model solved with computationally involving density functional methods [11].

To improve this simple-minded approach further one has to consider that the electron is not necessarily emitted at the pulse peak, but anywhere else during the pulse with a probability proportional to $A_L(t)^{2n}$. In each case one can determine the favourable CE phase interval in which the electron is allowed to escape from the surface. Overlapping these intervals with their corresponding weights ($A_L(t)^{2n}$)

results in a histogram-like distribution (Fig. 2.) which is equivalent to the electron yield as a function of CE phase already computed with a radically different method based on the jellium model [11, 13]. The qualitative agreement of these two is the more remarkable. The maxima of electron emission peaks with respect to the CE phase are at the same positions ($-\pi/4$) and the modulation depth of the emitted current is also correct to within 10%. Deviation in terms of the shape of the CE phase dependence curve can only be observed for longer pulses and could be attributed to some artefact in our computation procedure given the irregular curve shapes towards longer pulse lengths and the unrealistically preserved, relatively high modulation depth.

3. Experimental Time-Resolved Investigations of MSPE

Testing these predictions could be carried out experimentally thanks to the existence of CE phase stabilized laser systems. Even though compelling evidence was shown in these experiments that the photoelectron emission process is governed not just by the field amplitude, but also by the actual waveform (or, in other words, the CE phase), observed modulation depths were well below the ones predicted by any of the models [12, 14]. This discrepancy remained to be resolved, so we carried out diagnostic measurements of the emission process with (non-phase-stabilized) few-cycle laser pulses. Standard characteristics, such as the intensity and polarization dependence of the emitted charge followed predictions and corresponded to the vectorial nature of MSPE, however, when a time-resolved interferometric autocorrelation measurement was carried out, interesting new effects emerged [14].

We used ultrashort, chirped-pulse-amplified Ti:sapphire laser pulses to carry out the measurements. After the prism-based pulse compressor ~ 25 fs-long (FWHM) pulses were generated with ~ 1.0 mJ pulse energy and a repetition rate of 1 kHz. The central wavelength was 800 nm. After a further pulse compression stage consisting of a Ne-filled, 1.0 m-long, 180 μm -core diameter hollow fibre under 1.5 bar gas pressure, the laser pulses were further shortened to a duration of 9.5 fs in our case with the aid of broadband chirped mirrors. (Further details of the laser system can be found in Ref. [17].) The pulse length at the output of the laser system was close to the transform limited one that can be inferred from the measured spectrum. There was some uncompensated higher order dispersion, but this should not influence major conclusions later on.

The above-described beam was sent into a Michelson interferometer the output of which was used to induce the MSPE process from a gold electrode enclosed in a sealed and evacuated glass tube. We restrict ourselves to moderate laser intensities, i.e. we remain within the perturbative regime excluding the possibility of tunnelling emission. The emitted electrons were collected by an anode to which an extraction voltage of 15 kV was applied. Due to the ~ 1.55 eV photon energy and the ~ 4.6 eV work function of the gold surface the electron emission is a third-order process and according to the simplified Sommerfeld model for metallic electrons the measured

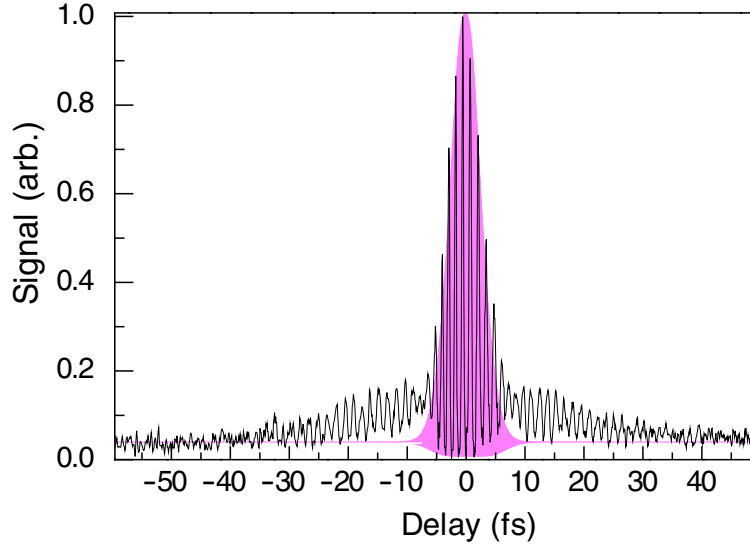


Fig. 3. Third-order autocorrelation curve of 9.5 fs-long laser pulses using MPSE form the gold surface as a third-order detector. The shaded background corresponds to the calculated envelope of the third-order autocorrelation function of a Gaussian pulse with the same pulse duration

photocurrent should show a $j \propto |E_{\perp}|^{2n}$ dependence on the field component perpendicular to the surface. Therefore one can record third-order autocorrelation curves by measuring the signal for each delay between the two interfering pulses. Surprisingly the observed autocorrelation trace (solid curve in Fig. 3.) differs significantly from the expected one (which is acquired by calculating the autocorrelation function of a 9.5 fs-long Gaussian pulse and it is represented by the shaded are in the figure).

The most conspicuous feature is the 25 fs-long pedestal of the measured curve which corresponds to some temporal lengthening in the emission process. Alternatively, one can say that this indicates that three-photon electron emission does not take place instantaneously, but through some intermediate states with ultrafast dynamics. This assumption is further supported by the fact that at sufficiently long delays, however, the curve converges to the expected background value which should have a ratio of 1:32 to the peak in case of a third-order process. Moreover, similar observations are also known from time-resolved two-photon-induced photoelectron emission experiments carried out with longer pulses and other materials [18, 19]. The decoherence this temporal lengthening indicates would obviously impair the predicted CE phase-sensitivity of the photoemission process and it is a sign of ultrafast hot electron dynamics. Based on this first measurement further investigations are needed to identify exactly the underlying physical effects for ex-

ample potential involvement of image states in the process or to see whether it is the polycrystalline nature of the surface that results in this distortion not predicted by recent models. Experiments with a single-crystal gold surface kept under ultrahigh vacuum conditions involving shorter (6 fs) pulses are under way.

4. Discussion, Summary and Outlook

Once the processes leading to the measured distorted autocorrelation curve are identified, they can be incorporated with more accuracy into the phenomenological model described in Section 3. Until then, however, also based on a similar phenomenological approach one could also include some effects of the indicated non-instantaneous emission in this model. For example, one could assume that the emission process is initiated overwhelmingly around the peak of the pulse, but free electron motion near the surface governed by the field of the pulse starts slightly later depending on the lifetime of the intermediate states involved. This lifetime can be roughly estimated from the measured autocorrelation curve. Quantification of this is a bit more demanding task, since not just the distribution of the starting points of the photoemission process has to be taken into account (as done for the calculations resulting in Fig. 2), but the temporal distribution of the duration, too, which the electron spends in some hot electron state characterized by a certain lifetime. More accurate analyses could be carried out by a similar Bloch-equation method as described in Ref. [18], however, since there are more possible emission channels than for a two-photon process, this seems to be a computationally involved task.

In summary, we have performed estimations of the sensitivity of photoelectron emission to the carrier-envelope phase of a laser pulse for different pulse lengths using a simple phenomenological model. The results of these simulations are in remarkable qualitative agreement and in good quantitative agreement with the conclusions of previous, more rigorous calculations for few-cycle laser pulses interacting with a gold surface. As a result of experiments on MSPE of gold induced by few-cycle laser pulses in order to study its characteristics under these new conditions we observed that the intensity and polarization dependences did agree well with previous observations performed with longer pulses, while the high-order autocorrelation curve reveals a certain time lengthening in the interaction process indicating ultrafast level dynamics in the femtosecond range.

Further theoretical and experimental study of this phenomenon is necessary, because such a lengthening may strongly decrease the efficiency of the dependence of the multi-photon processes in general on the carrier-envelope phase of few-cycle laser pulses. Once the necessary conditions for high-contrast, CE-phase sensitive laser–solid interaction is observed the way for constructing a compact, single-shot, solid-state-based CE phasemeter is cleared which immediately brings benefits to the technology at the core of attosecond science.

Acknowledgement

Gy. Farkas would like to thank the support of the Hungarian Scientific Research Fund (Contract No. T-048324) during the experiments.

References

1. T. Brabec and F. Krausz, *Rev. Mod. Phys.* **72** (2000) 545.
2. M. Hentschel et al., *Nature* **414** (2001) 509.
3. Gy. Farkas and Cs. Tóth, *Phys. Lett. A* **168** (1992) 447.
4. R. Szipőcs and A. Köházi-Kis, *Appl. Phys. B* **65** (1997) 115.
5. P. Agostini and L. DiMauro, *Rep. Prog. Phys.* **67** (2004) 813.
6. S.P.D. Mangles et al., *Nature* **431** (2004) 535; C.G.R. Geddes et al., *Nature* **431** (2004) 538; J. Faure et al., *Nature* **431** (2004) 541.
7. A. Pukhov and J. Meyer-ter-Vehn, *Appl. Phys. B* **74** (2002) 355.
8. K. Yamane et al., *Conf. on Lasers and Electro-optics (CLEO)*, 2004, Postdeadline paper CPDC2; see also B. Schenkel et al., *Opt. Lett.* **28** (2003) 1987.
9. S.T. Cundiff, *J. Phys. D* **35** (2002) R43.
10. A. Baltuska et al., *Nature* **421** (2003) 611.
11. Ch. Lemell, X.-M. Tong, F. Krausz and J. Burgdörfer, *Phys. Rev. Lett.* **90** (2003) 076403.
12. A. Apolonski, P. Dombi, G.G. Paulus, M. Kakehata, R. Holzwarth, Th. Udem, Ch. Lemell, K. Torizuka, J. Burgdörfer, T.W. Hänsch and F. Krausz, *Phys. Rev. Lett.* **92** (2004) 073902.
13. P. Dombi et al., *New J. Phys.* **6** (2004) 39.
14. P. Dombi, F. Krausz and Gy. Farkas, submitted for publication.
15. P.B. Corkum, *Phys. Rev. Lett.* **71** (1993) 1994.
16. M. Lewenstein, Ph. Balcou, M.Yu. Ivanov, A. L'Huillier, P.B. Corkum, *Phys. Rev. A* **49** (1994) 2117.
17. S. Sartania, Z. Cheng, M. Lenzner, G. Tempea, Ch. Spielmann, F. Krausz and K. Ferencz, *Opt. Lett.* **22** (1997) 1562.
18. T. Hattori, Y. Kawashima, M. Daikoku, H. Inouye and H. Nakatsuka, *Jpn. J. Appl. Phys.* **39** (2000) 4793.
19. M.J. Weida, S. Ogawa, H. Nagano and H. Petek, *J. Opt. Soc. Am. B* **17** (2000) 1443.

